

NC STATE UNIVERSITY

Wideband Vibrational Energy Harvesting:
A Nonlinear Approach using
Magnetostrictive Material (MsM)



By: Chris Page

Date: March 21, 2013

Abstract

Table of Contents

| | |
|----------------------------|-------------------------------------|
| Nomenclature | 4 |
| Introduction | 5 |
| Background | Error! Bookmark not defined. |
| Theory | 14 |
| Experimental Setup..... | 24 |
| Discussion of Results..... | 28 |
| Conclusion..... | 35 |
| References | 36 |
| Appendix | 45 |

Nomenclature

Introduction

Structural Health Monitoring is a relatively new field that has become popular in many industries including aerospace, civil, and automotive; and similar schemes have become integral in environmental and animal observations and studies. Today, wireless sensors monitor the surrounding environment by collecting relevant measurements and transmitting the data via radio frequency (RF) transmission to a base station where it is processed further and interpreted. Such measurements include, but are not limited to: pressure, temperature, seismic vibration, wind speed/direction, heartrate, gps location, etc. Wireless sensor networks are used in aircraft, civil structures (bridges, etc.), military surveillance, personal tracking devices, industrial process monitoring, environment/habitat monitoring, traffic control, and so on. Because these networks are wireless, their power source is usually a battery with finite life available. Recently, the field of energy harvesting to provide additional power has become a topic of interest. Using the surrounding environment as a power source can extend the life of the battery if not provide enough recharging power to keep the battery fully charged indefinitely. However, batteries also have a finite number of charge/discharge cycles, meaning they will eventually have to be replaced. In some applications this is quite difficult as the individual nodes may be inaccessible or simply densely distributed in which case it becomes expensive to replace batteries. There is a large push to develop energy harvesting methods that do not require a battery for built-up energy storage. Imagine if the harvesting device can collect enough energy *quickly* enough to power the sensor directly. Therefore, in any setup, the power available and required is of important consideration.

Most applications require a relatively low duty cycle as the pertinent information to measure does not change rapidly. This means that each sensor node spends most of its lifetime in standby mode, resulting in a typical power requirement of less than 1 mW (Roundy *et al.*, 2005a). There are several sources of energy available from the surrounding environment. Table (1) gives an overview of such sources and their typical capabilities and characteristics.

Table 0: Energy and power sources comparisons (Roundy *et al.*, 2005a)

| Power source | Power (μW)/ cm^3 | Energy (Joules)/ cm^3 | Power (μW)/ cm^3 /yr | Secondary storage needed? | Voltage regulation | Commercially available |
|----------------------------------|--|--------------------------------|--|---------------------------|--------------------|------------------------|
| Primary battery | N/A | 2,880 | 90 | No | No | Yes |
| Secondary battery | N/A | 1,080 | 34 | N/A | No | Yes |
| Micro fuel cell | N/A | 3,500 | 110 | Maybe | Maybe | No |
| Ultracapacitor | N/A | 50-100 | 1.6-3.2 | No | Yes | Yes |
| Heat engine | 1E6 | 3,346 | 106 | Yes | Yes | No |
| Radioactive (^{63}Ni) | 0.52 | 1,640 | 0.52 | Yes | Yes | No |
| Solar (outside) | 15,000* | N/A | N/A | Usually | Maybe | Yes |
| Solar (inside) | 10* | N/A | N/A | Usually | Maybe | Yes |
| Temperature | 40*† | N/A | N/A | Usually | Maybe | Soon |
| Human power | 330 | N/A | N/A | Yes | Yes | No |
| Air flow | 380‡ | N/A | N/A | Yes | Yes | No |
| Pressure variation | 17§ | N/A | N/A | Yes | Yes | No |
| Vibrations | 375 | N/A | N/A | Yes | Yes | No |

* Measured in power per square centimeter, rather than power per cubic centimeter.

† Demonstrated from a 5 °C temperature differential.

‡ Assumes an air velocity of 5 m/s and 5 percent conversion efficiency.

§ Based on 1 cm³ closed volume of helium undergoing a 10 °C change once a day.

For the applications at hand, the three most popular sources are solar (outside), air flow, and vibrations. It is widely known that solar provides the highest power density, however many applications are not conducive to using this source, especially indoor applications such as heartrate monitoring of a patient in a hospital. The use of air flow is also a popular energy harvesting method. Large wind turbines collect enough energy to power homes and even entire cities. On the other hand, this technology does not scale well and thus smaller versions do not provide the necessary energy at slow flow rates. And again, many applications do not have a potentially useful air flow source. Finally, vibrational energy harvesting has become a growing interest in this field of powering wireless sensors. Vibrations occur in almost all structures and environments. The kinetic energy available to harvest is dependent on the vibration frequency and amplitude. Examples of this type of harvester include the Seiko Kinetic watch and the shake-driven flashlight.

Background

Vibrational energy harvesting is accomplished using a proof mass that oscillates relative to the surrounding environment which is converted using various electromechanical devices. For the most basic devices, the mass is chosen such that vibration resonates with the surroundings at one of the low-order modes involved. Roundy *et al.* (2005a) developed a 1 cm³ prototype design that produced 375 μW of power from 2.5 m/s² vibrations at 120 Hz. In general, power densities in the range of 50-400 μW/cm³ have been achieved. These levels of power density are well suited for wireless sensor node applications. This same group has summarized a table of common vibration sources, provided here in Table (2).

Table 0: Sources of mechanical vibrations (Roundy *et al.*, 2003; Leland *et al.*, 2004)

| Vibration Source | Acceleration (m/s ²) | Frequency (Hz) | Vibration Source | Acceleration (m/s ²) | Frequency (Hz) |
|-----------------------------------|----------------------------------|----------------|-----------------------------------|----------------------------------|----------------|
| Car engine compartment | 12 | 200 | HVAC vents in office buildings | 0.2-1.5 | 60 |
| Base of 3-axis machine tool | 10 | 70 | Windows next to a busy road | 0.7 | 100 |
| Blender casing | 6.4 | 121 | CD on notebook computer | 0.6 | 75 |
| Clothes in dryer | 3.5 | 121 | Second story floor of busy office | 0.2 | 100 |
| Persons nervously tapping heels | 3 | 1 | Wooden deck with people walking | 1.3 | 385 |
| Car instrument panel | 3 | 13 | Bread maker | 1.03 | 121 |
| Door frame just after door closes | 3 | 125 | Washing machine | 0.5 | 109 |
| Small microwave oven | 2.5 | 121 | Refrigerator | 0.1 | 240 |

The two important characteristics of a vibrating source are the maximum acceleration and the frequency at which that acceleration occurs. Since most ambient vibrations have very low accelerations, the frequency becomes the design factor to look at. Current harvesters are designed to resonate with this frequency. However, at low vibration frequencies, it is very difficult to achieve resonance without increasing device size substantially (Roundy *et al.*, 2003). As the source deviates from this resonant frequency, the harvester's efficiency drops dramatically.

The conversion from kinetic energy to electrical energy is accomplished based on the specific electromechanical device used. William and Yates (1995) have proposed a generic model for a vibration to electrical energy converter. The converter is modeled as a single degree of freedom mass-spring-damper system as described in Figure (1).

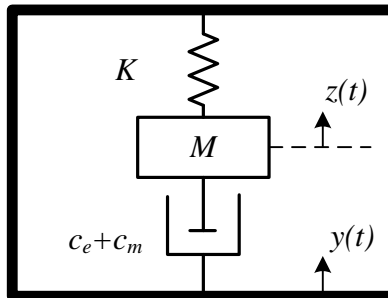


Figure 0: Generic Model for a Vibration to Electrical Energy Converter

In such a system, the damper represents loss of mechanical energy. In a vibration based energy harvester, since the energy converted to electrical form is the loss of kinetic energy from the mechanical system, the conversion mechanism can be treated as an electrical damping effect on the mechanical system. Consequently, the equivalent mass spring damper system can be expressed by the following equation

$$M\ddot{z} + (c_e + c_m)\dot{z} + Kz = -M\ddot{y} \quad (0.1)$$

where M is the vibrating effective mass

y is the input displacement due to vibration

z is the spring deflection opposing the input displacement

c_e is the electrical damping coefficient

c_m is the mechanical damping coefficient; K is the spring constant.

The electrical power converted from the mechanical system is equal to the electrical damping loss of the mechanical system by c_e . The harvested electrical power can be expressed as (Roundy *et al.*, 2004)

$$P_e = \frac{1}{2} c_e \dot{z}^2 = \frac{M \zeta_e \omega_n \omega^2 \left(\frac{\omega}{\omega_n} \right)^4 Y^2}{\left(2 \zeta_T \frac{\omega}{\omega_n} \right)^2 + \left(1 - \left(\frac{\omega}{\omega_n} \right)^2 \right)^2} \quad (0.2)$$

where $\zeta_T = \zeta_e + \zeta_m$ is the combined damping ratio, and ζ_e , ζ_m are the electrical and mechanical damping ratio. The relation between the damping ratio and damping coefficient is $c = 2M\omega_n\zeta$.

If the device is designed to resonate at the natural frequency ω_n , i.e. $\omega = \omega_n$, the electrical power can be maximized to

$$P_e = \frac{1}{2} c_e \dot{z}^2 = \frac{M \zeta_e \omega_n^3 Y^2}{4 \zeta_T^2} = \frac{M \zeta_e A^2}{4 \omega_n \zeta_T^2} \quad (0.3)$$

where $A = \omega_n^2 Y$ is the acceleration magnitude of input vibrations.

Energy is converted whenever work is done by the input vibration force against the electrical damping force. The electrical damping effect is achieved using an electromechanical transducer. Such a transducer can be implemented using one of the following four conversion mechanisms: electromagnetic converter, electrostatic converter, piezoelectric converter and magnetostrictive converter. This work utilizes the latter.

Magnetostrictive Materials (MsM) have a characteristic known as the Villari effect. When the material undergoes strain its magnetic properties change. If the MsM experiences a constantly changing strain field, its magnetic field is constantly changing. This magnetic flux can be converted to electrical energy using a pickup coil and Faraday's law of induction. The linearized material behavior can be expressed using

$$\begin{aligned} B &= \mu^T H + d \sigma \\ \varepsilon &= d H + s^H \sigma \end{aligned} \quad (0.4)$$

where B is magnetic flux density

μ^T is permeability under constant stress

H is magnetic field intensity

d is piezomagnetic coefficient of MsM

σ is mechanical stress

ε is mechanical strain

s^H is elastic compliance under constant magnetic field

The magnetostriction coefficient is defined as the fractional change in length of the material in response to increase in the magnetization of the material from zero to the saturation value (Hyperphysics, 2009). Many ferromagnetic materials such as cobalt and nickel exhibit magnetostriction, however their conversion efficiency is very low. In 2007, Lei Wang proposed the use of amorphous Metglas 2605SC alloy for vibration energy harvesting. Metglas 2605SC has a conversion efficiency of 97%. An electromechanical circuit model was presented for an MsM based energy harvester. Maximum output power was 200 μW when the harvester was excited by 58 Hz vibrations. The output voltage was only 0.15 V; less than the forward voltage drop of a diode. When an 8 layers MsM device is driven by 1.1 kHz vibration, the output power to a 3 F supercapacitor is 576 μW . Figure (2) below shows his device; a cantilever beam with the thin Metglas bonded to the surface. This figure also shows the pick up coil.

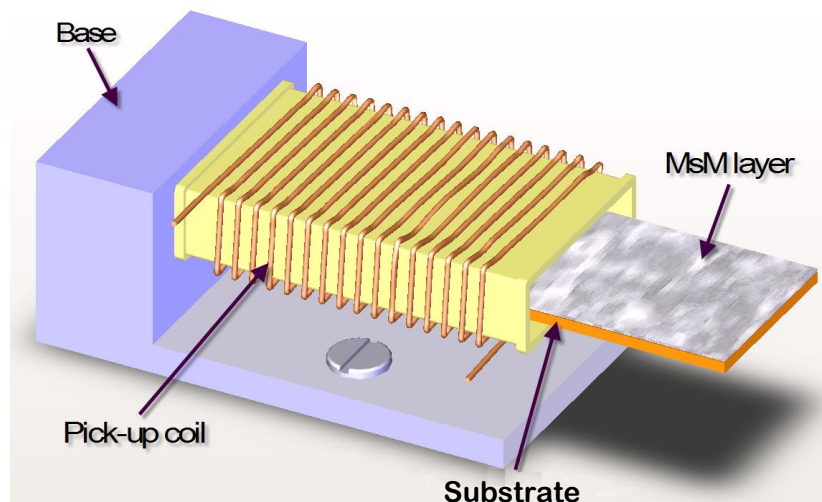


Figure 2: Vibrational Energy Harvesting Device used by Wang(2007)

This previous work has two notable characteristics relevant to the work presented here. First, Wang(2007) explored a fixed-frequency harvester. In other words, as mentioned before, the device is tuned for resonance with the vibrational source. Also, the device underwent small deflections classified as within the linear region of stress/strain. As pointed out in (Roundy *et al.*, 2003, 2005a), the output power from such converters falls off very quickly even if there is a slight mismatch between the natural frequency of the device and the input vibration frequency. Therefore, it is very essential that the natural frequency of the device closely matches the vibration frequency. In most of the environments, depending on the operating conditions, the

frequency of the driving vibration may change over time. In order to solve this obstacle, researchers have explored devices that can harvest a wider bandwidth of vibrating frequencies. This is often referred to as wideband energy harvesting. Furthermore, one of the more popular strategies investigated are devices with nonlinear characteristics. Soliman *et al.* (2008) developed a wideband electromagnetic converter using piecewise-linear oscillators instead of linear oscillator to sense input vibrations. The proposed oscillator used a stopper that moved along a track in the horizontal direction and is maintained at a constant height above a cantilever beam. As the input oscillations increase, the stopper changes the effective length of the beam. Simulation results showed that 30% more energy was collected using the stopper over a 13.8 Hz range around the natural frequency of the converter. The work presented here involves structural nonlinearity; as the MsM and its substrate are loaded until buckled, and then they are vibrated. In this regime, the deflection of material is nonlinearly related to the additional applied load past critical buckling load. A generic graphical representation of this is shown in Figure (3).

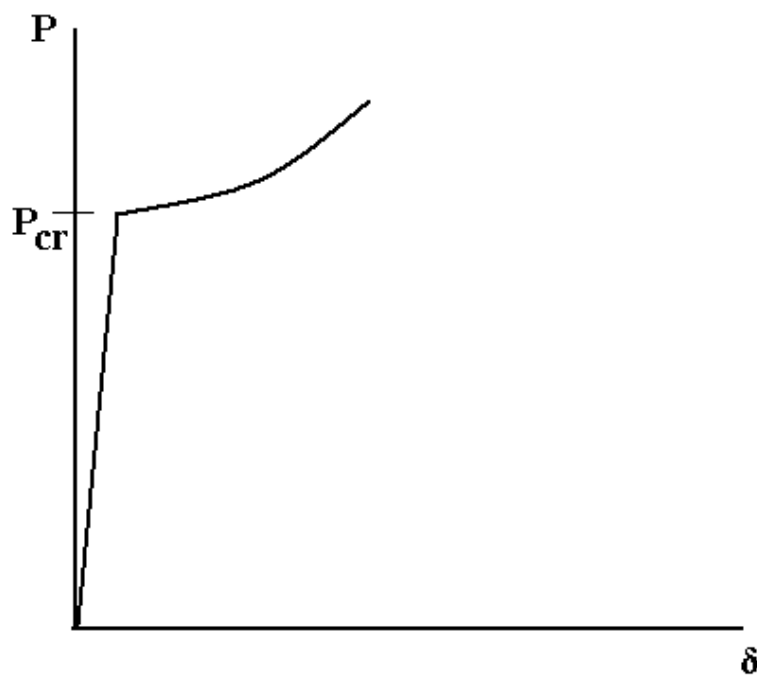


Figure 3: Illustration of Beam Deflection Pre- and Post- Buckled

Assuming a non-perfect beam, there exists very little deflection up until the critical load is applied. After this point the beam is considered first-mode buckled and the deflection increases drastically with additional loading. More notable, this new region is nonlinear. The next step is to

investigate how working in this regime affects the characteristics of the beam's stress/strain fields and therefore the magnetic field of the MsM.

Nonlinear Theory

We must first begin with the simplified linear model of the harvester. The linearized one-dimensional magnetomechanical constitutive equation of MsM material is similar to that of uniaxial piezoelectric material (IEEE Standard, 1991). It follows a piezomagnetic law (IEEE Standard, 1991). It can be expressed in the following form.

$$\begin{Bmatrix} \varepsilon \\ B \end{Bmatrix} = \begin{bmatrix} s^H & d \\ d^* & \mu^T \end{bmatrix} \begin{Bmatrix} \sigma \\ H \end{Bmatrix} \quad (0.1)$$

where ε and σ are mechanical strain and stress respectively; B and H are magnetic flux density and field intensity respectively; s^H is the elastic compliance under constant magnetic field; μ^T is the permeability under constant stress; d and d^* are two magnetomechanical coefficients. These two coefficients (i.e., d and d^*) can be determined experimentally with the following definitions.

$$d = \left. \frac{\partial \varepsilon}{\partial H} \right|_{\sigma}$$

$$d^* = \left. \frac{\partial \varepsilon}{\partial H} \right|_H$$

Error!
Reference source
not found.)

where subscript σ and H refer to the measurements under constant stress and constant magnetic field intensity respectively. Note that d and d^* can be considered to be equal for small strains (Wang, 2007).

Rearranging Eq. (0.1) by switching the position of ε and σ leads to the following form:

$$\begin{Bmatrix} \sigma \\ B \end{Bmatrix} = \begin{bmatrix} E^H & -e \\ e^* & \mu^S \end{bmatrix} \begin{Bmatrix} \varepsilon \\ H \end{Bmatrix} \quad (0.2)$$

where $E^H = 1/S^H$ is Young's modulus or elastic modulus under constant magnetic field; $\mu^S = \mu^T - d \cdot d^* / S^H$ is the permeability under constant strain; coefficients e and e^* can be calculated by:

$$e = E^H d \quad (0.3a)$$

$$e^* = E^H d^* \quad (0.3b)$$

An important figure of merit for MsM is the material coupling coefficient, k , which is defined as (Du Traemolet de Lacheisserie, 1993; Engdahl, 2000; Wang, 2007):

$$k = \frac{\mathcal{E}_{mM}}{\sqrt{\mathcal{E}_m \mathcal{E}_M}} \quad (0.4)$$

where $\mathcal{E}_m = \sigma s^H \sigma / 2$, $\mathcal{E}_M = H \mu^T H / 2$ and $\mathcal{E}_{mM} = \sigma d H / 2$ are the mechanical, magnetic, and mutual magnetoelastic energy respectively. Substituting the definitions of \mathcal{E}_m , \mathcal{E}_M and \mathcal{E}_{mM} into Eq. (0.4) (Wang, 2007), one can obtain:

$$k = \frac{d}{\sqrt{\mu^T s^H}} \quad (0.5)$$

For the nonlinear case, the beam must be re-examined and linear assumptions are re-evaluated. Nonlinearities in structural mechanics come up in many different ways including material, geometric, inertia, and friction nonlinearities (Emam, 2002). Geometric nonlinearities originate from nonlinear strain-displacement relationships. Sources of this type of nonlinearity include midplane stretching, large curvatures of structural elements, and large rotation of elements. Because of the midplane stretching, the governing equation of a buckled beam

possesses cubic nonlinearities. It should be noted here that the boundary conditions for this study include simply supported and clamped-clamped. Both setups involve applying *axial* preload until the beam buckles. The nonlinear responses of buckled beams have been investigated by many researchers in the past century. Burgreen (1951) investigated experimentally and analytically the free vibrations of a simply supported buckled beam using single-mode discretization. He presented that the natural frequencies of the buckled beams depend on the amplitude of vibration. Easley (1964a, 1964b) investigated the forced vibrations of the buckled beams and obtained similar forms of the governing equations for simply supported and clamped-clamped buckled beams using single-mode discretization. Abu-Ryan *et al.* (1993) investigated the nonlinear dynamics of a simply supported buckled beam using single-mode approximation to a principal parametric resonance. They obtained a sequence of supercritical period-doubling bifurcations leading to chaos and snapthrough motions. This regime promises high changes in strain fields within the beam.

The prototype of the wideband energy harvester is shown in Figure(4). The clamped-clamped beam consists of Metglas layers which are bonded on a brass substrate and is wound by a pick-up coil. This buckled beam was originally flat and has been compressed past the critical buckling load P_{cr} to a static deflection position w_0 by an axial force P with clamped ends. The buckled beam is excited by the base motion y . The nonlinear MsM energy harvester is operating around the first buckling mode of the clamped-clamped beam.

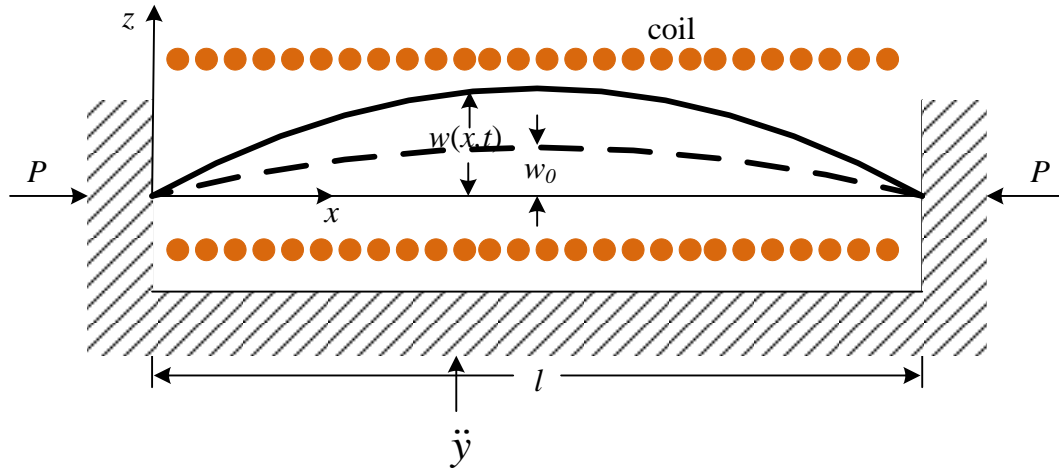


Figure 4: Nonlinear MsM energy harvester

Assume that axes x and z are in horizontal and vertical directions respectively as shown in Figure(4). The source vibration y is in the z direction. The beam configuration is a unimorph structure with MsM layers on the top side of the substrate. Both the substrate and MsM laminate have the same width b and length l and their thicknesses are t_s and t_M respectively. To derive the model of the nonlinear vibration of the wideband MsM energy harvester, some assumptions are made. First, the in plane deformation is ignored. Second, the transverse shear strains are ignored. Consequently, the rotation of the cross section is due to bending only. The last assumption is that no transverse normal strains are considered. Therefore, the beam can be modeled according to the Euler-Bernoulli beam theory.

To derive the equations of motion and associated boundary conditions for continuous system, the extended Hamilton principle is developed.

$$\int_{t_0}^{t_f} (\delta T - \delta V + \delta W_M + \delta W_{nc}) dt = 0 \quad (2)$$

where T is the kinetic energy, V is the potential energy, also called elastic energy, W_M is the magnetic energy, W_{nc} is the non-conservative work, and t_0 , t_f the initial and final times respectively.

The kinetic energy is given by

$$T = \frac{1}{2} \int_0^l m_s \left(\frac{\partial w}{\partial t} \right)^2 dx + \frac{1}{2} \int_0^l m_M \left(\frac{\partial w}{\partial t} \right)^2 dx = \frac{1}{2} \int_0^l m \left(\frac{\partial w}{\partial t} \right)^2 dx \quad (0.6)$$

where subscripts s and M indicate the substrate and MsM layer, respectively. m is the mass per unit length.

The first variation of the kinetic energy can be obtained by (Emam, 2002)

$$\begin{aligned} \int_{t_0}^{t_f} \delta T dt &= \int_{t_0}^{t_f} \delta \left[\frac{1}{2} \int_0^l m \left(\frac{\partial w}{\partial t} \right)^2 dx \right] dt = \int_{t_0}^{t_f} \int_0^l m \frac{\partial w}{\partial t} \frac{\partial}{\partial t} \delta w dx dt \\ &= m L \left[\frac{\partial w}{\partial t} \delta w \right]_{t_0}^{t_f} - \int_{t_0}^{t_f} \int_0^l m \frac{\partial^2 w}{\partial t^2} \delta w dx dt = - \int_{t_0}^{t_f} \int_0^l m \frac{\partial^2 w}{\partial t^2} \delta w dx dt \end{aligned} \quad (0.7)$$

where the first term vanishes by virtue of Hamilton's principle.

The potential energy due to bending is given by

$$V_b = \frac{1}{2} \int_{V_s} \varepsilon \sigma_s dV_s + \frac{1}{2} \int_{V_M} \varepsilon \sigma_M dV_M \quad (0.8)$$

According to the Euler-Bernoulli beam theory,

$$\varepsilon = -z \frac{\partial^2 w}{\partial x^2} \quad (0.9)$$

According to the Hooke's law, the stress of the substrate is given by

$$\sigma_s = E_s \varepsilon \quad (0.10)$$

The second equation in Eq. (0.2) can be rewritten as

$$\sigma_M = E^H \varepsilon - eH \quad (0.11)$$

Assuming the solenoid coil is long and neglecting fringing effect, magnetic field intensity H can be expressed by Ampere's law

$$H = \frac{N}{l} i \quad (0.12)$$

Substituting Eqs. (0.9) ~ (0.12) into Eq. (0.8) yields

$$\begin{aligned} V_b &= \frac{1}{2} \int_{V_s} E_s z^2 \left(\frac{\partial^2 w}{\partial x^2} \right)^2 dV_s + \frac{1}{2} \int_{V_M} E^H z^2 \left(\frac{\partial^2 w}{\partial x^2} \right)^2 dV_M + \frac{1}{2} \int_{V_M} eH z \left(\frac{\partial^2 w}{\partial x^2} \right) dV_M \\ &= \frac{1}{2} EI \int_0^l \left(\frac{\partial^2 w}{\partial x^2} \right)^2 dx + \frac{NdE^H A_M h_M}{2l} \int_0^l i \left(\frac{\partial^2 w}{\partial x^2} \right) dx \end{aligned} \quad (0.13)$$

where

$$EI = E_s \left(\frac{bt_s^3}{12} + A_s h_s^2 \right) + E^H \left(\frac{bt_M^3}{12} + A_M h_M^2 \right) \quad (0.14)$$

The potential energy due to the axial force P is given by (Emam, 2002)

$$V_a = -\frac{1}{2} P \int_0^l \left(\frac{\partial w}{\partial x} \right)^2 dx \quad (0.15)$$

The potential energy due to the midplane stretching is given by (Emam, 2002)

$$V_{st} = \frac{E_s A_s + E^H A_M}{8l} \left[\int_0^l \left(\frac{\partial w}{\partial x} \right)^2 dx \right]^2 = \frac{EA}{8l} \left[\int_0^l \left(\frac{\partial w}{\partial x} \right)^2 dx \right]^2 \quad (0.16)$$

where A_s and A_M are the cross section area of the substrate and the MsM layer, respectively.

$$EA = E_s A_s + E^H A_M \quad (0.17)$$

Therefore, the total potential energy can be expressed as

$$V = \frac{1}{2} EI \int_0^l \left(\frac{\partial^2 w}{\partial x^2} \right)^2 dx + \frac{NdE^H A_M h_M}{2l} \int_0^l i \left(\frac{\partial^2 w}{\partial x^2} \right) dx - \frac{1}{2} P \int_0^l \left(\frac{\partial w}{\partial x} \right)^2 dx + \frac{EA}{8l} \left[\int_0^l \left(\frac{\partial w}{\partial x} \right)^2 dx \right]^2 \quad (0.18)$$

$$\begin{aligned} \int_{t_0}^{t_f} \delta V = & \int_{t_0}^{t_f} \int_0^l \left\{ \left[EI \frac{\partial^4 w}{\partial x^4} + P \frac{\partial^2 w}{\partial x^2} - \frac{EA}{2l} \frac{\partial^2 w}{\partial x^2} \int_0^l \left(\frac{\partial w}{\partial x} \right)^2 dx \right] \delta w + \frac{NdE^H A_M h_M}{2l} i \delta \left(\frac{\partial^2 w}{\partial x^2} \right) \right. \\ & \left. + \frac{NdE^H A_M h_M}{2l} \frac{\partial^2 w}{\partial x^2} \delta i \right\} dx dt + \int_{t_0}^{t_f} \left\{ EI \frac{\partial^2 w}{\partial x^2} \delta \left(\frac{\partial w}{\partial x} \right) - \left[EI \frac{\partial^3 w}{\partial x^3} + P \frac{\partial w}{\partial x} \right. \right. \\ & \left. \left. - \frac{EA}{2l} \frac{\partial w}{\partial x} \int_0^l \left(\frac{\partial w}{\partial x} \right)^2 dx \right] \delta w \right\} dt \end{aligned} \quad (0.19)$$

The magnetic energy is given by

$$W_M = \frac{1}{2} \int_{V_M} BH dV_M = -\frac{NdE^H A_M h_M}{2l} \int_0^l i \left(\frac{\partial^2 w}{\partial x^2} \right) dx + \frac{\mu^s N^2 A_M}{2l^2} \int_0^l i^2 dx \quad (0.20)$$

$$\int_{t_0}^{t_f} \delta W_M = \int_{t_0}^{t_f} \int_0^l \left\{ -\frac{NdE^H A_M h_M}{2l} i \delta \left(\frac{\partial^2 w}{\partial x^2} \right) - \frac{NdE^H A_M h_M}{2l} \frac{\partial^2 w}{\partial x^2} \delta i + \frac{\mu^s N^2 A_M}{l^2} i \delta i \right\} dx dt \quad (0.21)$$

The nonconservative work is given by

$$\delta W_{nc} = \int_{t_0}^{t_f} \left\{ \int_0^l \left(q - c_m \frac{\partial w}{\partial t} \right) \delta w dx + \varphi_v \delta i \right\} dt \quad (0.22)$$

where q is a distributed load in the transverse direction, $\frac{d\varphi_v}{dt} = v$, and v is the applied voltage.

Substituting Eq. (0.7), Eq. (0.19), Eq. (0.21) and Eq. (0.22) into Eq. () yields

$$\begin{aligned}
& \int_{t_0}^{t_f} \int_0^l \left\{ \left[-m \frac{\partial^2 w}{\partial t^2} - EI \frac{\partial^4 w}{\partial x^4} - P \frac{\partial^2 w}{\partial x^2} + \frac{EA}{2l} \frac{\partial^2 w}{\partial x^2} \int_0^l \left(\frac{\partial w}{\partial x} \right)^2 dx + q - c_m \frac{\partial w}{\partial t} \right] \delta w \right. \\
& \quad - \frac{NdE^H A_M h_M}{l} i \delta \left(\frac{\partial^2 w}{\partial x^2} \right) \left. \right\} dx dt + \int_{t_0}^{t_f} \left\{ \int_0^l \left[-\frac{NdE^H A_M h_M}{l} \frac{\partial^2 w}{\partial x^2} \right. \right. \\
& \quad \left. \left. + \frac{\mu^s N^2 A_M}{l^2} i \right] dx + \varphi_v \right\} \delta i dt - \int_{t_0}^{t_f} \left\{ EI \frac{\partial^2 w}{\partial x^2} \delta \left(\frac{\partial w}{\partial x} \right) \right. \\
& \quad \left. - \left[EI \frac{\partial^3 w}{\partial x^3} + P \frac{\partial w}{\partial x} - \frac{EA}{2l} \frac{\partial w}{\partial x} \int_0^l \left(\frac{\partial w}{\partial x} \right)^2 dx \right] \delta w \right\} dt = 0
\end{aligned} \tag{0.23}$$

Because Eq. (0.23) must hold true for any arbitrary δw , δi , and $\delta(\partial w/\partial x)$, the integrand should be zero. As a result, the governing equations for the nonlinear MsM energy harvester are

$$\begin{aligned}
& \int_0^l \left\{ \left[-m \frac{\partial^2 w}{\partial t^2} - EI \frac{\partial^4 w}{\partial x^4} - P \frac{\partial^2 w}{\partial x^2} + \frac{EA}{2l} \frac{\partial^2 w}{\partial x^2} \int_0^l \left(\frac{\partial w}{\partial x} \right)^2 dx + q - c_m \frac{\partial w}{\partial t} \right] \delta w \right. \\
& \quad \left. - \frac{NdE^H A_M h_M}{l} i \delta \left(\frac{\partial^2 w}{\partial x^2} \right) \right\} dx = 0
\end{aligned} \tag{0.24a}$$

$$\int_0^l \left(-\frac{NdE^H A_M h_M}{l} \frac{\partial^2 w}{\partial x^2} \right) dx + \frac{\mu^s N^2 A_M}{l} i + \varphi_v = 0 \tag{0.24b}$$

The boundary conditions are

$$EI \frac{\partial^2 w}{\partial x^2} = 0 \quad \text{or} \quad \frac{\partial w}{\partial x} \quad \text{at} \quad x = 0 \quad \text{and} \quad x = l \tag{0.25}$$

and

$$EI \frac{\partial^3 w}{\partial x^3} + P \frac{\partial w}{\partial x} - \frac{EA}{2l} \frac{\partial w}{\partial x} \int_0^l \left(\frac{\partial w}{\partial x} \right)^2 dx = 0 \quad \text{or} \quad w = 0 \quad \text{at} \quad x = 0 \quad \text{and} \quad x = l \tag{0.26}$$

Assume the buckled beam has been compressed past the critical buckled load, P_{cr} , to a static deflection w_0 . Following the Rayleigh-Ritz method, $w(x,t)$ can be given by

$$w(x,t) = w_0(x) + \sum_{r=1}^{N_r} \phi_r(x) r_r(t) = w_0(x) + \Phi(x) \mathbf{r}(t) \quad (0.27)$$

where $w_0(x)$ is the static deflection of the buckled beam, $\Phi(x) = [\phi_1(x), \dots, \phi_{N_r}(x)]$ is modal vector of the beam, and $\mathbf{r}(t) = [r_1(t), \dots, r_{N_r}(t)]^T$ is generalized coordinate vector.

The axial force P is defined by

$$P = P_{cr} + \frac{EA}{2l} \int_0^l \left(\frac{\partial w_0}{\partial x} \right)^2 dx \quad (0.28)$$

and the initial static deflection w_0 satisfies

$$EI \frac{\partial^4 w_0}{\partial x^4} + P_{cr} \frac{\partial^2 w_0}{\partial x^2} = 0 \quad (0.29)$$

where P_{cr} is the fundamental buckling load of a clamped-clamped beam.

Instituting Eqs. (0.27) ~ (0.29) into Eq. (0.24), the governing equations can be obtained by

$$\begin{aligned} & \left(\int_0^l m \Phi^T(x) \Phi(x) dx \right) \ddot{\mathbf{r}}(t) + EI \left(\int_0^l \Phi^T(x) \Phi^{iv}(x) dx \right) \mathbf{r}(t) + P_{cr} \left(\int_0^l \Phi^T(x) \Phi''(x) dx \right) \mathbf{r}(t) \\ & - \frac{EA}{2l} \left\{ \int_0^l \int_0^l \left[\Phi'^T(x) \Phi'(x) \mathbf{r}(t) \mathbf{r}^T(t) + 2 \Phi'^T(x) w_0'(x) \mathbf{r}^T(t) \right] dx \right\} \Phi^T(x) (\Phi''(x) \mathbf{r}(t) \\ & + w_0''(x) dx) \} + c_m \left(\int_0^l \Phi^T(x) \Phi(x) dx \right) \dot{\mathbf{r}}(t) + \frac{NdE^H A_M h_M}{l} \left(\int_0^l \Phi''^T(x) dx \right) \mathbf{i} \\ & = q \int_0^l \Phi^T(x) dx \end{aligned} \quad (0.30a)$$

$$\mathbf{v} = \frac{NdE^H A_M h_M}{l} \left(\int_0^l \Phi''(x) dx \right) \dot{\mathbf{r}}(t) - \frac{\mu^s N^2 A_M}{l} \mathbf{i} \quad (0.30b)$$

Looking at Eq. (0.30), the buckled MsM energy harvester has a cubic nonlinear term for $r(t)$ in time which makes wideband design possible.

Experimental Setup

The first experimental apparatus designed was for a simply-supported beam configuration. This boundary condition is highly idealized, however the devices' design attempted to model this as closely as possible. Figure (5) and (6) show the conceptual boundary conditions and the actual device's, respectively.

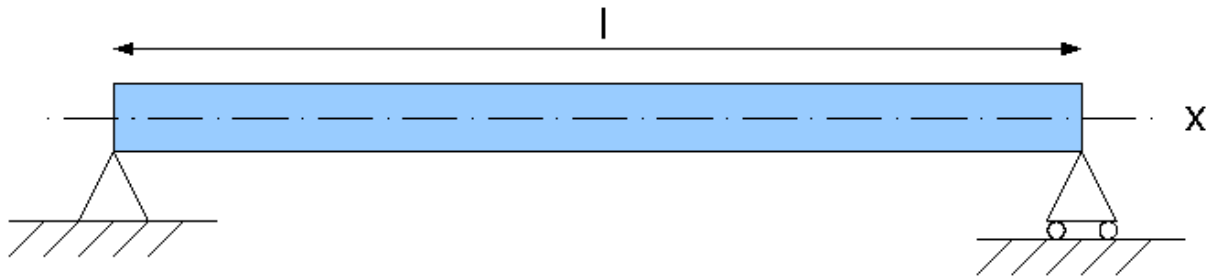


Figure 5: Conceptual Illustration of Simply Supported Beam



Figure 6: Experimental Model of Simply Supported Beam

The beam is compressed by and angled piece of aluminum on each side. Notches are cut out of these to allow for rotation of the beam as it deflects in the buckled regime. This eliminates any

reaction moments at the boundary. One of these angles is clamped in place while the other is allowed to slide along a track while the preload is being administered. Once the desired amount of load is accomplished, this angle is clamped as well and the test is begun. Figure (7) shows the full Solidworks model of this.

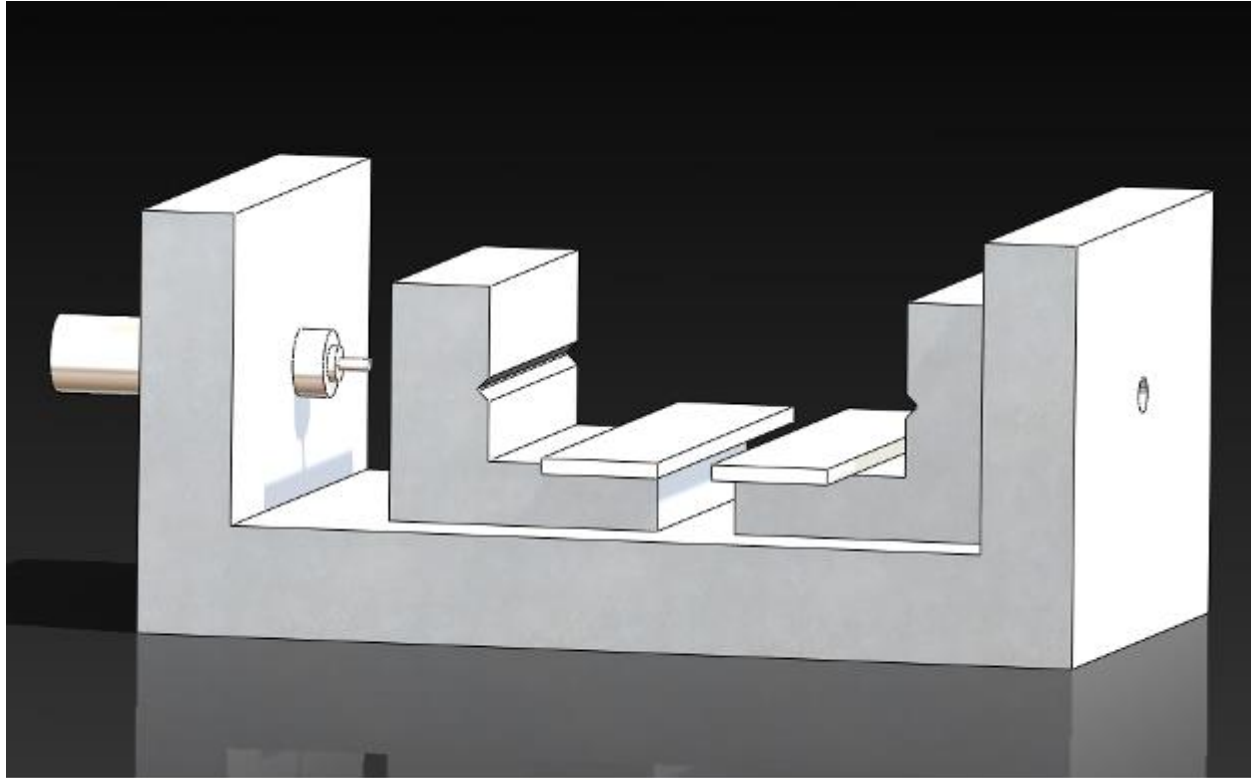


Figure 7: Simply Supported Test Apparatus

The shortcomings of this device is that it cannot perfectly mimic the simply supported boundary conditions. In order to accomplish this, one of the angles must be fixed and one must be free to slide back and forth *while* the test is being run. Also, the notch helps to eliminate reaction moments, but any misalignment in the machining of the track or the notch *or* the test beam and the beam and the angle do not make a perfect contact, especially in the in-plane direction This results in some initial twist of the beam. Finally, in order to test the effectiveness of the buckled scenario, we must first run the test with no axial preload. For the simply supported case, this means zero reaction in the x direction and zero in the negative y direction (vertical). In the test environment, this is impossible. The baseline, therefore, will have just enough axial preload to hold the beam to the device.

Next, the clamped-clamped boundary condition was explored, because this proved to be easier to accomplish experimentally. Figure (8) and (9) show the conceptual boundary conditions and the actual device's, respectively.

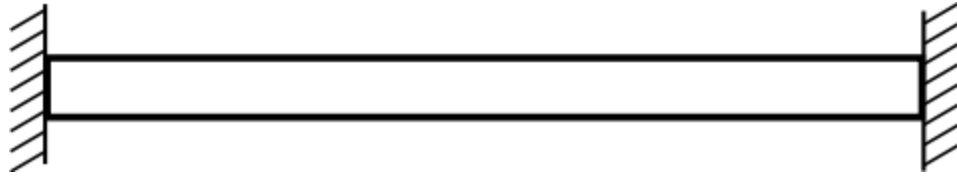


Figure 8: Conceptual Illustration of Clamped-Clamped Beam

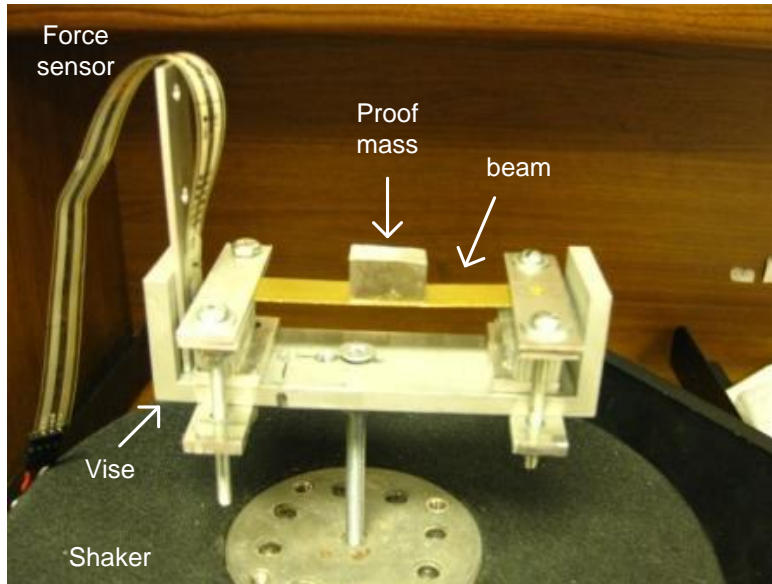


Figure 9: Test Apparatus for Clamped Clamped Beam

The same basic apparatus was used as before, but the angled aluminum was replaced with two clamps. The only obstacles in this setup are ensuring that the beam is placed in the clamps orthogonal to the clamp edges and that there is even pressure across the plane. Using clamping metal that has high stiffness and tightening the screws on either side of the beam an even amount helps to ensure this. Also, in this scheme, a proof mass is used; but not to match the resonant frequencies. Here it is used simply to lower the natural frequency of the device as buckling a clamped beam increases this characteristic over 20 times the baseline values.

Auxiliary test equipment include a FlexiForce piezoresistive force sensor from Tekscan, Inc., mounted at one end of the device. A micrometer is used to apply the preload, as well as measure the axial displacement. A power amplifier with high drive strength, 2125MB from MB Electronics, Inc. and a vibration shaker VTS100-8 from Vibration Test Systems, Inc. were used to drive the apparatus. The unimorph beam was comprised of a brass substrate and four layers of cast Metglas2605 SA1 on the top surface. An Agilent 33120A function/arbitrary waveform generator creates a sinusoidal signal that is sent to a KH Krohn-hite 7602M wideband amplifier

to drive the vibration shaker. The MsM prototype device is mounted on top of the shaker. The output signal from the MsM is measured using a Tektronix DPO2024 digital phosphor oscilloscope. The photograph of the actual experimental setup is shown in **Error! Reference source not found.**(10). Table (3) shows the relevant values of the harvesting device.

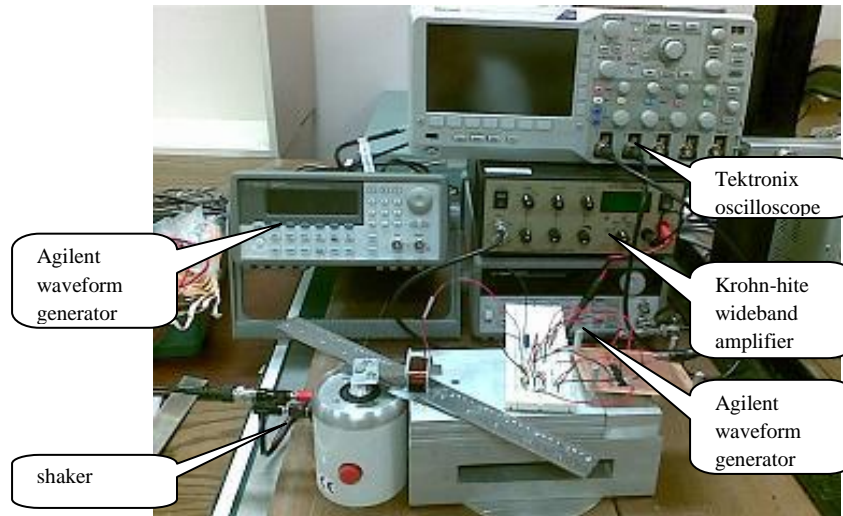


Figure 10: Supporting Electronics for Testing

Table 3: Parameters of the clamped-clamped beam

| Parameter | Value |
|----------------------------------|------------|
| Length | 59.24mm |
| Width | 12.5mm |
| Thickness of the brass shim | 0.19mm |
| Thickness of Metglas (one layer) | 0.022mm |
| Total thickness of the beam | 0.31mm |
| Young's modulus of Metglas | 100~110GPa |
| Young's modulus of brass | 100~110GPa |
| Proof mass | 12.95g |
| Turns of the coil | 3000 |

Discussion of Results

Experiments were carried out to study the nonlinearity of the prebuckled beam and the postbuckled beam under the compressive axial preload and heavy proof mass. The nominal peak acceleration of the driving vibrations used in the experiments was approximately 38 m/s^2 . The axial preload was carried from 0 N to 31 N in step of approximately 4 N. The natural frequency of the device, the bandwidth, the open circuit voltage and the peak output power were measured for each level of preload. The preload was gradually increased until the unimorph entered the plastic region. When the unimorph was close to the plastic region, some amount of irreversible deformation existed. The power output reduced to zero. Therefore, the unimorph had to be discarded and was not used for subsequent measurements.

First, the simply supported buckled beam proved to be unusable in this study because of the obstacles discussed earlier. During testing, the possible introduction of twist and the lack of correct boundary conditions led to measurements that were not higher than the generic noise floor of the measurement equipment. Therefore, no results are presented here.

The clamped clamped condition was easier to control, however there still exists some disparity between the experimental observations and the theory. From calculations, the theoretical critical buckling load is around 31 N, however in the experiment the unimorph buckled below the theoretical critical buckling load and entered the plastic region when the load exceeded the theoretical critical buckling load. The heavy proof mass in the middle of the beam applies additional midplane stretching thereby reducing the critical buckling load from the axial force.

The following factors may affect the measurement results and mismatch the theoretical results:

- The unimorph is not a true long slender beam since the ratio of the unimorph's length to the width is not large enough.
- The length of the unimorph may change slightly for different preload.
- Locally stiff regions were formed during the machining process and due to the mass bonded on the unimorph.
- To apply the preload and to measure it, some part of the beam must be outside the clamps. As a result, the actual beam length is longer than the effective beam length. The friction that exists between the part of the beam outside the clamps and the force sensor or the force applying apparatus can affect the end conditions.

- The vibrations affect the clamping setup. This causes change in the applied axial force to the beam and also affects the end conditions.

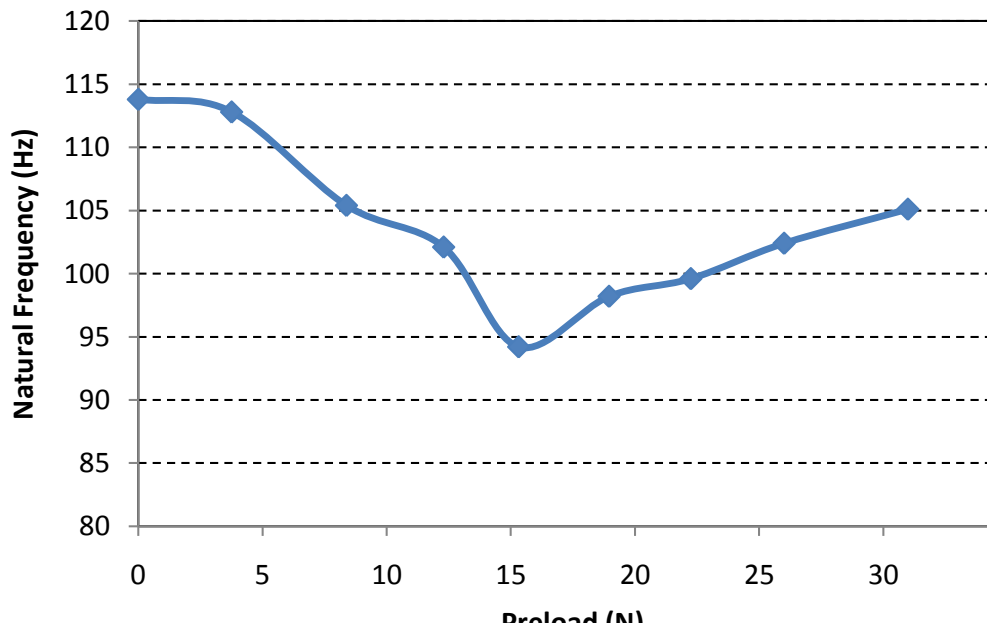


Figure 0.1. Natural frequency versus preload

The open-circuit natural frequency was measured for each level of preload by varying the frequency of the driving vibrations manually. Figure 0.1 shows the effects of compressive axial preload on natural frequency for the clamped-clamped MsM generator. For the 12.95 g proof mass, the natural frequency reduces from 113.8 Hz to 94.2 Hz first and then increases to 105.1 Hz as the preload is increased. As mentioned by Leland, E.S. and Wright, P.K. (2006) that the compressive axial preload can adjust the natural frequency of a simply supported beam below the unloaded natural frequency, the compressive axial preload lowers the natural frequency of a clamped-clamped beam before the beam buckles. According to the linear theory, the natural frequency becomes zero as the compressive preload reaches the critical buckling load. As predicted in Eq. **Error! Reference source not found.**, the natural frequency of the postbuckled beam increases for higher buckling level (i.e. higher preload). In the experiment, the unimorph buckled when preload reached around 15 N.

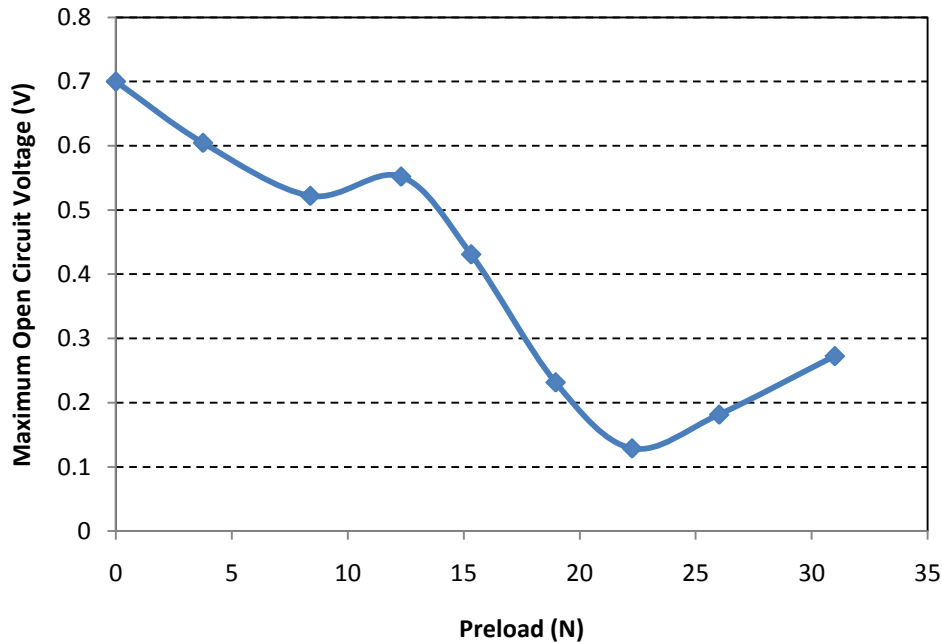
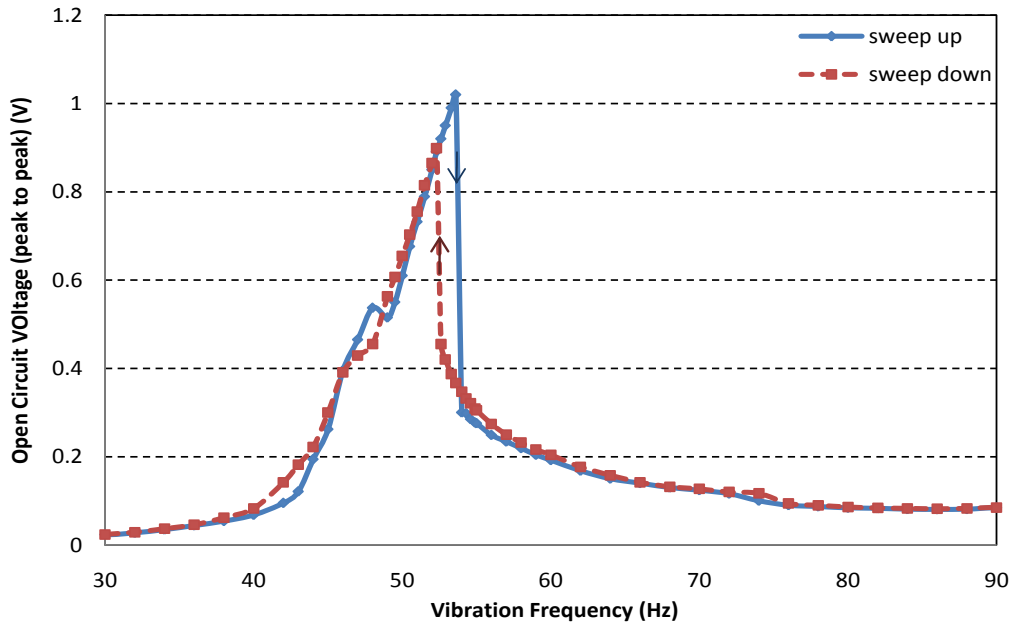


Figure 0.2. Maximum open circuit voltage versus the compressive axial preload

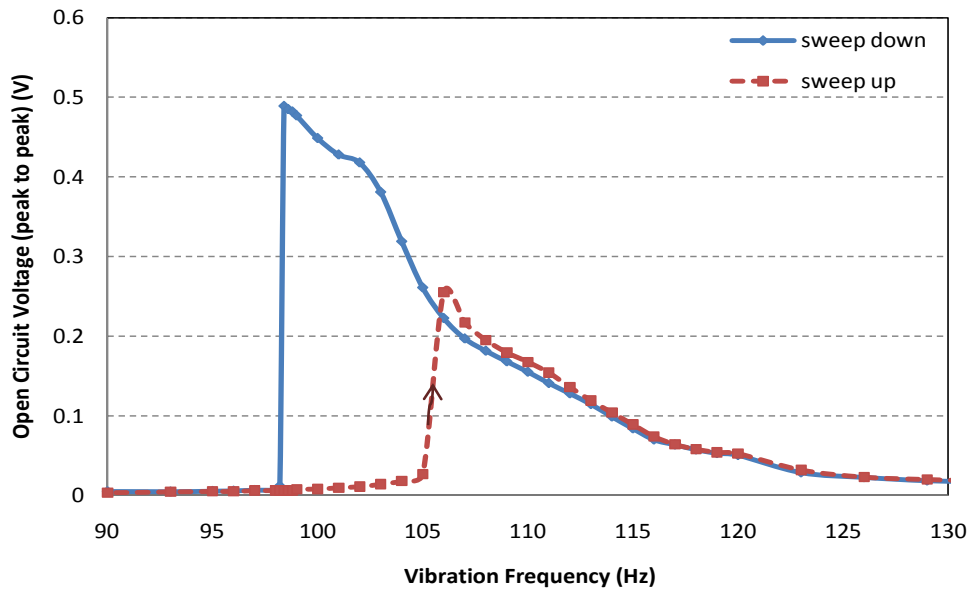
The maximum open circuit voltage was measured for each level of preload when the clamped-clamped beam was operating at the open-circuit natural frequency. Figure 0.2 illustrates the effect of the compressive axial preload on the maximum open circuit voltage. Before the beam buckles, the maximum open circuit voltage decreases from 0.7 V to 0.5 V as the preload is increased. After the beam buckles, the maximum open circuit voltage continues to decrease up to 0.13V first and then increases to 0.27 V. The relationships described in Eq. **Error! Reference source not found.**) and Eq. **Error! Reference source not found.**), however, suggest that the maximum open circuit voltage should increase at higher preload. For the postbuckled problem, the theoretical results about the effect of the buckling level on the open circuit voltage have been predicted in Section **Error! Reference source not found.**. This mismatch between the theoretical results and the experimental results might be explained by the increase in the device damping at higher levels of preload (Leland, E.S. and Wright, P.K., 2006).

Figure 0.3 shows the open circuit voltage as a function of the input vibration frequency. With the heavy proof mass, the clamped-clamped beam shows nonlinearity under both zero and 19 N preload. The effects of the nonlinearity include the change in the natural frequency and the bending of the frequency response. When the clamped-clamped beam is under zero preload, the resonance peak bends to higher frequencies as shown in Figure 0.3a. The midplane stretching, caused by the heavy proof mass, results in the hardening effect. Heavier proof mass will cause larger bending of the frequency response. For the postbuckled clamped-clamped beam, the resonance peak bends to lower frequencies as shown in Figure 0.3b. Here, the softening effect caused by the axial load dominates the hardening effect caused by the heavy proof mass. As a

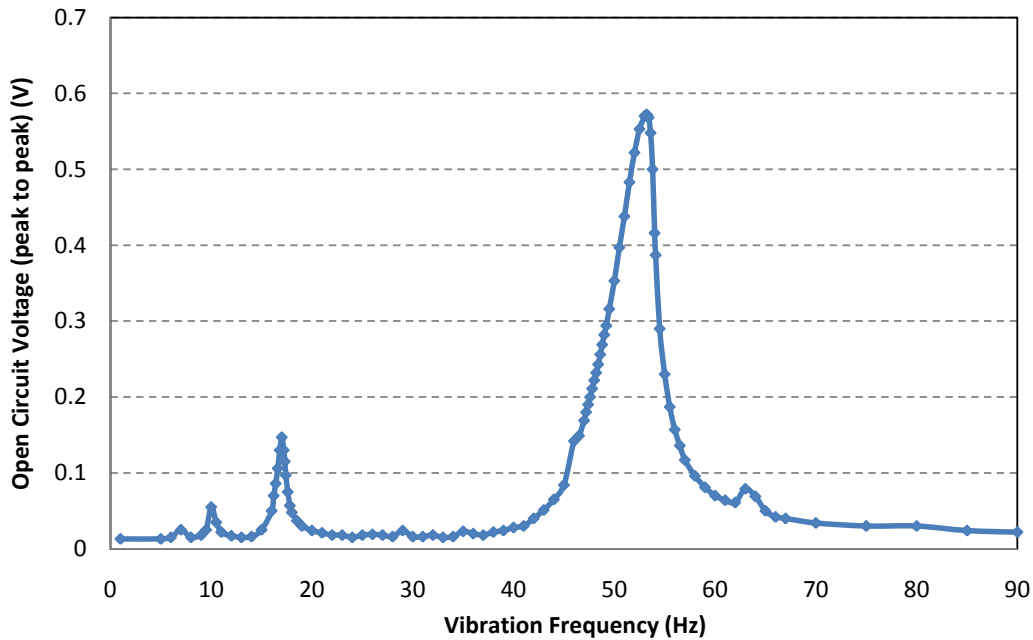
comparison, the nearly linear response can be seen for the cantilever beam as shown in Figure 0.3c. However, for the large excitation acceleration, the cantilever beam will also show some amount of nonlinearity. For a highly nonlinear system, hysteresis appears in the frequency domain depending on the direction of vibration frequency sweep. This can be observed in the experiment. The jump phenomenon that the open circuit voltage undergoes, a sudden discontinuous jump near resonance happened as shown in Figure 0.3a and Figure 0.3b.



(a)



(b)



(c)

Figure 0.3. Peak to peak open circuit voltage as a function of input vibration frequency (a) when no axial preload is applied to the clamped-clamped beam; (b) when 19 N axial preload is applied to the clamped-clamped beam; (c) for linear cantilever beam

The nonlinearity represented as the bending of the frequency response indicates the possibility that the nonlinear system has a wider band than the linear system. Figure 0.4 shows the relationship between the 3dB bandwidth and the compressive axial preload. For the prebuckled beam, the bandwidth is nearly constant since the dominant nonlinearity is caused by the constant proof mass. For the postbuckled beam, the bandwidth changes since the nonlinearity due to the varying axial load becomes dominant. The maximum bandwidth of 9.3 Hz can be obtained for the postbuckled clamped-clamped beam in the experiment.

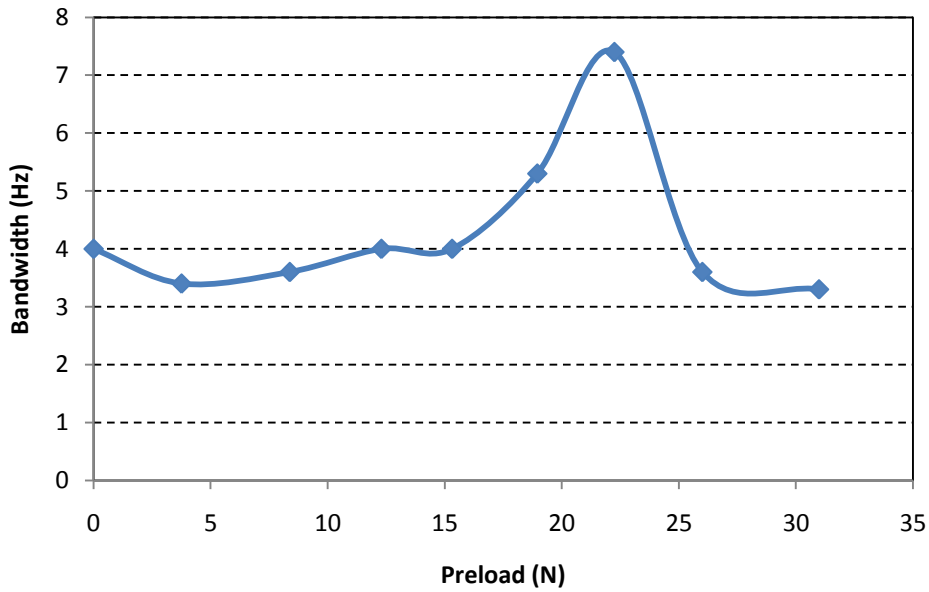


Figure 0.4. Bandwidth versus preload

The output power was calculated from the measured RMS voltage drop across a known resistance. The maximum output power for each level of preload was measured when the beam was operating at the natural frequency and drove an optimum resistive load. Figure 0.5 shows the maximum output power as a function of the preload. The maximum output power has the same behavior against the preload as that of the maximum open circuit voltage. The maximum output power for each level of preload is in the range of 49 μW and 3 μW . In contrast to the relationship between the bandwidth and the preload, the damping reduces the output power while increases the bandwidth. From Figure 5.12 and 5.13, it can be seen that the damping will increase the bandwidth at the expense of the output power.

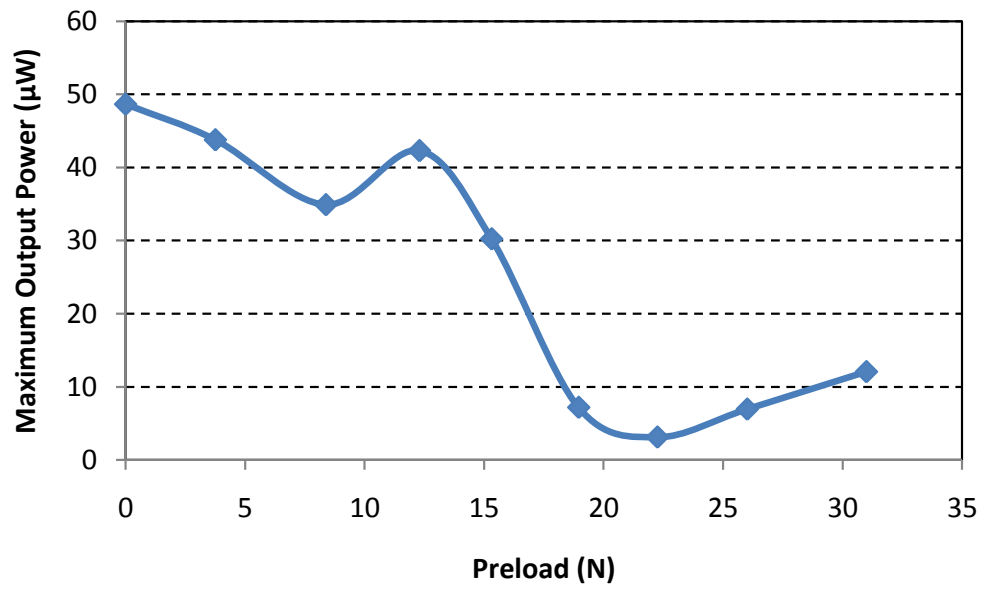


Figure 0.5. Maximum output power versus preload

Conclusion

The primary goal of this work was to investigate and prove that applying a buckling load to a vertically vibrating MsM beam can increase its energy harvesting bandwidth. The single-mode approximation shows that there exists a cubic term in the governing equations of the beam which proves, theoretically, that wideband energy harvesting is possible. The next step was to prove this theory with experimental results. Careful design of an accurate test apparatus took place, striving to mimic conceptual boundary conditions and to remain congruent with the assumptions made in the theory.

For the simply supported scenario, the boundary conditions were highly idealized and thus required careful attention and furthermore, precise machining. Even with these steps taken, the experiments involving this setup were inconclusive as the open-circuit voltages were not high enough to distinguish from the existing noise involved with the measurement equipment. It was quickly decided that this experiment was too difficult to control and time would be better spent with the clamped clamped boundary condition.

The clamped experiments proved to be somewhat more successful, although it should be noted that it was quickly apparent that these tests are very dependent on matching the experimental setup with the conceptual assumptions. A slight difference in this results in only mediocre results. With that said, we were able to observe some signs that applying a preload increases the bandwidth of the energy harvester. As noted before, this comes with the price of reducing the output power due to increased mechanical damping.

Future work should include a redesign of the test apparatus. Finer precision in machining and preparation can eliminate the twist involved in the simply supported case. Also, as discussed earlier, the simply supported boundary condition involves one fixed side and one side on frictionless rollers. This can be more closely mimicked by placing the moveable angle on a track bearing and by placing a spring in between the angle and the micrometer which applies the load. This will allow for the application of a buckling load while also allowing the boundary condition to move in the x direction as the beam vibrates, which could allow the beam to snapthrough the undeflected position into a negatively buckled geometry; and then back again. This will reduce the mechanical damping and may in fact produce more output power.

References

- Abou-Rayan, A. M., Nayfeh, A. H., and Mook, D. T. (1993). "Nonlinear response of a parametrically excited buckled beam," *Nonlinear Dynamics*, vol. 4, pp. 499-525, 1993.
- Amirtharajah, R. and Chandrakasan, A.P. (1998). "Self-powered signal processing using vibration-based power generation," *IEEE Journal of Solid State Circuits*, vol. 33, No. 5, pp. 687-695, 1998.
- Arakawa, Y., Suzuki, Y., and Kasagi, N. (2004). "Micro seismic electret generator using electrets polymer film," in *Proc. 4th Int. Workshop Micro and Nanotechnology for Power Generation and Energy Conversion Applicat. Power MEMS*, Kyoto, Japan, pp. 187-190, 2004.
- Baker, R.J. (2008). *CMOS Circuit Design, Layout and Simulation*, John Wiley & Sons Pub. Hoboken, NJ 2008.
- BlazeLabs, (2009). <http://blazelabs.com/e-exp15.asp>
- Blevins, R. D. (1995). *Formulas for Natural Frequency and Mode Shape*, Krieger Pub., Malabar, Fla, 1995.
- Burgreen, D. (1951). "Free vibration of a pin-ended column with constant distance between pin ends," *Journal of Applied Mechanics*, vol. 18, pp. 135-139, 1951.
- Challa, V. R., Prasad, V. R., Shi, Y. and Fisher, F. T. (2008). "A vibration energy harvesting device with bidirectional resonance frequency tunability," *Smart. Mater. Struct.* 17015035, 2008.
- Charnegie D., (2005), Frequency tuning concepts for piezoelectric cantilever beams and plates for energy harvesting, B.S thesis, 2005.
- Ching, N. N. H., Wong, H. Y., Li, W. J., Leong, P. H. W., and Wen, Z. (2001). "A laser-micromachined vibrational to electrical power transducer for wireless sensing systems," in *Proc. 11th Int. Conf. Solid-State Sensors*, 2001.
- Cottone, F., Vocca, H. and Gammaitoni, L. (2009). "Nonlinear energy harvesting". *Phys. Rev. Lett.*, 102, 080601, 2009.
- Davino, D., Giustiniani, A. and Visone, C. (2009). "Capacitive load effects on a magnetostrictive fully coupled energy harvesting device," *IEEE Transactions on Magnetics*, vol. 45, No. 10, Oct. 2009.
- Despesse, G., Chaillout, J., Jager, T., Leger, J. M., Vassilev, A., Basrou, S., and Charlot, B. (2005). "High damping electrostatic system for vibration energy scavenging," in *Proc. Joint Conf. Smart Objects Ambient Intell.-Innov. Context-Aware Services: Usages Technol.*, France, pp. 283-286, 2005.
- Dong, Z. and Allen, P.E. (2002). "Low-voltage supply independent CMOS bias circuit," *IEEE 45th Midwest Symposium on Circuits and Systems*, vol. 3, pp. III-568- III-570, 2002.
- Douglas, J. et al. (2005). *Fluid Mechanics*, 5th ed. Harlow, U.K.: Pearson Prentice-Hall, 2005.

Du Trâemolet de Lacheisserie E. (1993). *Magnetostriction: Theory and Applications of Magnetoelasticity*. Boca Raton: CRC Press; 1993.

Eisley, J. G. (1964a). "Large amplitude vibration of buckled beams and rectangular plates," *AIAA Journal*, vol. 2, pp. 2207-2209, 1964.

Eisley, J. G. (1964b) "Nonlinear vibration of beams and rectangular plates," *ZAMP*, vol. 15, pp. 167-175, 1964.

El-Hami, M., Glynne-Jones, P., James, E., Beeby, S., White, N. M., Brown, A. D., Ross, J. N. and Hill, N. (2000). "A new approach towards the design of a vibration-based microelectromechanical generator," in *Proc. 14th Eur. Conf. Solid-State Transducers, Eurosensors XIV*, Copenhagen, Denmark, pp. 483-486, Aug. 2000.

Elvin, N. G., Elvin, A. A., and Spector, M. (2001). "A self-powered mechanical strain energy sensor." *Smart Materials & Structures*, 10(2), 293-299, 2001.

Emam, S. A. (2002). *A Theoretical and Experimental Study of Nonlinear dynamics of Buckled Beams*, PhD. Thesis, 2002.

Emam, S. A. and Nayfeh, A. H. (2003). "Nonlinear dynamics of a buckled beam subjected to a primary-resonance excitation", *Nonlinear Dynamics*, vol. 15, pp. 155-177, 2003.

Engdahl, G. (2000). *Handbook of Giant Magnetostrictive materials*. San Diego, Calif.: Academic; 2000.

Engineeringtoolbox, (2009) http://www.engineeringtoolbox.com/young-modulus-d_417.html, 2009.

Erickson, R. W. and Maksimovic, D. *Fundamentals of Power Electronics*, 2nd ed. Springer, USA, 2001.

Erturk, A., Hoffman, J. and Inman, D. J. (2009). "A piezomagnetoelastic structure for broadband vibration energy harvesting," *Appl. Phys. Lett.*, 94, 254102, 2009.

FCC, (2002a). http://wireless.fcc.gov/siting/FCC_LSGAC_RF_Guide.pdf, May 2003.

FCC, (2002b). <http://ftp.fcc.gov/Bureaus/Wireless/Orders/1995/fcc95041.txt>, May 2003.

Friedman, D., Heinrich, H. and Duan, D. W. (1997). "A low-power CMOS integrated circuit for field-powered radio frequency identification," *Proceedings, IEEE Solid-State Circuits Conference*, pp. 294 – 295, 474, 1997.

Gendelman, O., Manevitch, L. I., Vakakis, A. F., and Bergman, L. A. (2003). "A degenerate bifurcation structure in the dynamics of coupled oscillators with essential stiffness nonlinearities," *Nonlinear Dynam.*, 33 (1), pp. 1-10, 2003.

Guan, M. J. and Liao, W. H. (2008). "Characteristics of energy storage devices in piezoelectric energy harvesting systems," *Journal of Intelligent Material Systems and Structures*, vol. 19, No. 6, 671-680, 2008.

- Guyomar, D., Badel, A., Lefeuvre, E. and Richard, C. (2005). "Toward energy harvesting using active materials and conversion improvement by nonlinear processing," *IEEE Transactions on Ultrasonics, Ferroelectrics, and Frequency Control*, vol. 52, No. 4, pp. 584-595, 2005.
- Guyomar, D. and Lallart, M. (2009). "Mechanical to electrical energy conversion enhancement and self-powered wireless applications," *Smart Structures and Materials*, pp. 91-105, 2009.
- Hammond, K., Lai, E., Leland, E., Mellers, S., Steingart, D., Carleton, E., Reilly, B., Baker, J., Otis, B., Rabaey, J., Culler, D., and Wright, P. (2005). "An integrated node for energy-scavenging sensing, and data-transmission: Applications in medical diagnostics," in *Proc. 2nd Int. Workshop Wearable Implantable Body Sensor Netw.*, Imperial College London, 2005.
- Hitachi Unveils Smallest RFID Chip. (2003). *RFID Journal*, March 14, 2003.
- Holmes, P. J. (1979). "A nonlinear oscillator with a strange attractor," *Philosophical Transactions of Royal Society of London A*, vol. 292, pp. 419-448, 1979.
- Holmes, P. J. and Moon, F. C. (1983). "Strange attractor and chaos in nonlinear mechanics," *Journal of Applied Mechanics*, vol. 50, pp. 1021-1032, 1983.
- Hu, Y., Xue, H. and Hu, H. (2007). "A piezoelectric power harvester with adjustable frequency through axial preloads," *Smart Materials and Structures*, 16, pp. 1961-1966, 2007.
- Huang W S, Tzeng K E, Cheng M C and Huang R. S. (2003a). "Design and fabrication of a vibrational micro-generator for wearable MEMS," *MEMS Proc. Eurosensors XVII (Guimaraes, Portugal)* pp 695-7, 2003.
- Huang, J., O'Handley, R. C., and Bono, D. (2003b). "New, high-sensitivity, hybrid magnetostrictive/electroactive magnetic field sensors." *Proceedings of SPIE*, 5050, 229-237, 2003.
- Hyperphysics, (2009). <http://hyperphysics.phy-astr.gsu.edu/hbase/solids/magstrict.html>, 2009.
- IEEE Standard Board. (1991). IEEE standard on magnetostrictive materials: piezomagnetic nomenclature. *IEEE STD 319-1990*. 1991.
- Inman, D. J. (2001). *Engineering vibration*, Prentice Hall, Upper Saddle River, N.J, 2001.
- James, E. P., Tudor, M. J., Beeby, S. P., Harris, N. R., Glynne-Jones, P., Ross, J. N. and White, N. M. (2004). "An investigation of self-powered systems for condition monitoring applications," *Sensors Actuators A, Phys.*, vol. 110, pp. 171-176, Feb. 2004.
- James, M.L., Smith, G. M., Wolford, J. C. and Whaley, P. W. (1994). *Vibration of Mechanical and Structural Systems*, Harper Collins College Publishers, New York, NY 1994.
- Kasyap, A., Lim, li-Song, Johnson, D., Horowitz, S., Nishida, T., Ngo, K., Sheplak, M. and Cattafesta, L. (2002). "Energy reclamation from a vibrating piezoceramic composite beam," *9th International Congress on Sound and Vibration*. Orlando, FL, July 2002.

- Kerschen, G., Vakakis, A. F., Lee, Y. S., McFarland, D. M., Kowtko, J., and Bergman, L. A. (2005) "Energy transfers in a system of two coupled oscillators with essential nonlinearity: 1 : 1 resonance manifold and transient bridging orbits," *Nonlinear Dynam.*, 42, pp. 282–303, 2005.
- Kreider, W. and Nayfeh, A. H. (1998). "Experimental investigation of single-mode responses in a fixed-fixed buckled beam," *Nonlinear Dynamics*, vol. 15, pp. 155-177, 1998.
- Kulah, H. and Najafi, K. (2004). "An electromagnetic micro power generator for low-frequency environmental vibrations," *Micro Electro Mechanical Systems—17th IEEE Conf. on MEMS (Maastricht)* pp 237–40, 2004.
- Lallart, M., Magnet, C., Richard, C., Lefeuvre, E., Petit, L., Guyomar, D. and Bouillault, F. (2008a). "New synchronized switch damping methods using dual transformations," *Sensors and Actuator A: Physical* 143(2), pp. 302-314, 2008.
- Lallart, M., Garbuio, L., Petit, L., Richard, C. and Guyomar, D., (2008b). "Double synchronized switch harvesting (DSSH): a new energy harvesting scheme for efficient energy extraction," *IEEE Trans. Ultrason. Ferroelect. Freq. Contr.* 55(10), pp. 2019-2130, 2008.
- Lallart, M. and Guyomar, D. (2008c). "An optimized self-powered switching circuit for non-linear energy harvesting with low voltage output," *Smart Material and Structures* 17 (2008).
- Lee S. H. (2001). "Development of high-efficiency silicon solar cells for commercialization," *Journal of the Korean Physical Society*, vol.39, no.2, pp.369-73, Aug. 2001.
- Lee, Y. S., Kerschen, G., Vakakis, A. F., Panagopoulos, P., Bergman, L., and McFarland, D. M. (2005). "Complicated dynamics of a linear oscillator with a light, essentially nonlinear attachment," *Physica D*, 204 (1–2), pp. 41–69, 2005.
- Lefeuvre, E., Badel, A., Richard, C., and Guyomar, D. (2005). "Piezoelectric energy harvesting device optimization by synchronous electric charge extraction," *J. Intell. Mater. Syst. Struct.*, vol. 16, pp. 865–876, Oct. 2005.
- Lefeuvre, E., Badel, A., Richard, C. and Guyomar, D. (2006). "A Comparison between Several Vibration-powered Piezoelectric Generators for Standalone Systems," *Sensors and Actuators A*, vol. 126, No. 2, pp. 405-416, 2006.
- Lefeuvre, E., Audigier, D., Richard, C. and Guyomar, D. (2007). "Buck-boost converter for sensorless power optimization of piezoelectric energy harvester," *IEEE Trans. Power Electronics*, pp. 2018-2025, Sep. 2007.
- Leland, E. S., Lai, E. M. and Wright, P. K. (2004). "A self-powered wireless sensor for indoor environmental monitoring," *Wireless Networking Symposium*, 2004.
- Leland, E.S. and Wright, P.K. (2006). "Resonance tuning of piezoelectric vibration energy scavenging generators using compressive axial preload," IOP Publishing, *Smart Mater.Struct.* 15 (2006) 1413-1420.

- Lesieutre, G. A. and Davis, C. L. (1997). "Can a coupling coefficient of a piezoelectric device be higher than those of its active material?" *J. Intell. Mater. Syst. Struct.* 8 859-67, 1997.
- Li, W. J., Ho, T. C. H., Chan, G. M. H., Leong, P. H. W. and Wong, H. Y. (2000). "Infrared signal transmission by a laser-micromachined vibration-induced power generator," in *Proc. 43rd IEEE Midwest Symp. Circuits Syst.*, vol. 1, pp. 236–239, Aug. 2000.
- Liu, L. and Yuan, F. G. (2008). "Wireless sensor with dual-controller architecture for active diagnosis in structural health monitoring", *Smart Materials and Structures*, vol. 17, No. 2, Article Number: 025016, 2008.
- Man, T.Y., Mok, P.K.T. and Chan, M. (2006). "A CMOS-control rectifier for discontinuous-conduction mode switching dc-dc converters," *IEEE International Solid-State Circuits Conference, Analog Techniques*, Feb.2006.
- Mann, B. P. and Sims, N. D. (2009). "Energy harvesting from the nonlinear oscillations of magnetic levitation". *J. Sound Vib.*, 319 pp. 515-530, 2009.
- McFarland, D. M., Bergman, L. A., and Vakakis, A. F. (2005). "Experimental study of nonlinear energy pumping occurring at a single fast frequency," *Intl. J. Non-linear Mech.*, 40 (6), pp. 891–899, 2005.
- McInnes, C. R., Gorman, D. G. and Cartmell, M. P. (2008). "Enhanced vibrational energy harvesting using nonlinear stochastic resonance". *J. Sound Vib.*, 38, pp. 655-662, 2008.
- Meningier, S., Mur-Miranda, J. O., Amirtharajah R., Chandrakasan, A. P. and Lang, J. (1999). "Vibration-to-electric conversion," *ISPLED99* San Diego, CA, USA, pp. 48 – 53, 1999.
- Miao, P., Mitcheson, P.D., Holmes, A.S., Yeatman, E., Green, T. and Stark, B. (2006). "MEMS inertial power generators for biomedical applications," *Microsyst. Technol.* vol. 12, No. 10-11, pp. 1079-1083, 2006.
- Mitcheson, P.D. et al. (2004). "Architectures for vibration-driven micropower generators," *J. Microelectromechanical Systems*, vol. 13, no. 3, 2004, pp. 429–440.
- Mitcheson, P.D., Yeatman, E.M., Rao, G.K., Holmes, A.S. and Green, T.C. (2008). "Energy harvesting from human and machine motion for wireless electronic devices," *Proceedings, IEEE*, vol. 96, No. 9, pp. 1457-1496, 2008.
- Mizuno, M. and Chetwynd, D. (2003). "Investigation of a resonance microgenerator," *J. Micromech. Microeng.* 13 209–16, 2003.
- Moehlis, J., Rogers, J. L., DeMartini, B. E. and Turner, K. L. (2009). "Exploiting nonlinearity to provide broadband energy harvesting," *ASME Dynamic Systems and Control Conference, DSCC-2542*, 2009.
- Moll, F. and Rubio, A. (2000). "An approach to the analysis of wearable body-powered systems," in *Proc. Mixed Design Integr. Circuits Syst. Conf.*, Gdynia, Poland, Jun. 2000.
- Moon, F. C. and Holmes, P. J. (1979). "A magnetoelastic strange attractor," *J. Sound Vib.* 65, 275, 1979.

Moon, F. C. (1980). "Experiments on chaotic motions of a forced nonlinear oscillator: strange attractor," *Journal of Applied Mechanics*, vol. 47, pp. 638-648, 1980.

Morris, D.J., Youngsman, J.M., Anderson, M.J. and Bahr, D.F. (2008). "A resonant frequency tunable, extensional mode piezoelectric vibration harvesting mechanism," IOP Publishing, *Smart Materials and Structures*, pp. 1-8, 2008.

Nayfeh, A. H. and Balachandran, B. (1995). *Applied Nonlinear Dynamics*, Wiley-Interscience, New York, 1995.

Ng, T. H., and Liao, W. H. (2005). "Sensitivity analysis and energy harvesting for a self-powered piezoelectric sensor," *J. Intell. Mater. Syst. Struct.*, vol. 16, no. 10, pp. 785-797, 2005.

Ottman, G. K., Hofmann, H. F., Bhatt, A. C., and Lesieutre, G. A. (2002). "Adaptive piezoelectric energy harvesting circuit for wireless remote power supply." *IEEE Trans. Power Electronics*, 17(5), 669-676, 2002.

Ottman, G. K., Hofmann, H. F. and Lesieutre, G. A. (2003). "Optimized piezoelectric energy harvesting circuit using step-down converter in discontinuous conduction mode," *IEEE Trans. Power Electronics*, 18(2), 696-703, 2003.

Panagopoulos, P. N., Vakakis, A. F., and Tsakirtzis, S. (2004). "Transient resonant interactions of linear chains with essentially nonlinear end attachments leading to passive energy pumping," *Intl. J. Solids Struct.*, 41 (22-23), pp. 6505-6528, 2004.

Paradiso, J.A. and Starner, T. (2005). "Energy scavenging for mobile and wireless electronics," *IEEE, Pervasive Computing*, vol. 4, pp. 18-27, Jan.-March, 2005.

Perpetuum Limited, (2008). http://www.perpetuum.co.uk/resource/PMG17-100_dsheets.pdf.

Quinn, D. D. (1997). "Resonance capture in a three degree-of-freedom mechanical system," *Nonlinear Dynamics*, 14, pp. 309-333, 1997.

Quinn, D. D., Vakakis, A. F., and Bergman, L. A. (2007). "Vibration-based energy harvesting with essential nonlinearities," *ASME International Design Engineering Technical Conferences, DETC2007-35457*, 2007.

Rand, R. H., Kinsey, R. J., and Mingori, D. L. (1992). "Dynamics of spinup through resonance," *Intl. J. Non-linear Mech.*, 27 (3), pp. 489-502, 1992.

Randall, J. F. (2003). *On ambient energy sources for powering indoor electronic devices*, PhD. Thesis, Ecole Polytechnique Federale de Lausanne, Switzerland, May 2003.

Roachman. (2003). <http://www.roachman.com/thermic/>, 2003

Roundy S., Wright P. K. and Pister K. S. J. (2002). "Micro-electrostatic vibration-to-electricity converters," *ASME IMECE*, Nov. 17-22, 2002.

- Roundy, S., Wright, P.K. and Rabaey, J. (2003). "A study of low level vibrations as a power source for wireless sensor nodes," *Computer Communications* 26 (2003) 1131-1144.
- Roundy, S., Wright, P. K., and Rabaey, J. M.(2004a). *Energy scavenging for wireless sensor networks: with special focus on vibrations*, Kluwer Academic, Boston, 2004.
- Roundy, S., Steingart, D., Frechette, L., Wright, P., and Rabaey, J., (2004b). "Power sources for wireless sensor nodes," *Lecture Notes in Computer Science*, vol. 2920/2004, pp. 1–17, Jan. 2004.
- Roundy, S., Leland, E. S., Baker, J., Carleton, E., Reilly, E., Lai, E. , Otis, B., Rabaey, J. M., Wright, P. K. and Sundararajan V. (2005a). "Improving power output for vibration-based energy scavengers," *IEEE Pervasive Computing*, vol. 4, pp. 28-36, Jan.-March, 2005.
- Roundy, S. and Zhang, Y. (2005b). "Toward self-tuning adaptive vibration based micro-generators," *Proceedings, SPIE*, vol. 5649, pp. 373-384, 2005.
- Saha, C., O'Donnell, T., Loder, H., Beeby, S. P. and Tudor, M. J. (2006) "Optimization of an electromagnetic energy harvesting device," *IEEE Trans. Magn.*, vol. 42, no. 10, pp. 3509–3511, 2006.
- Sari, I., Balkan, T. and Kulah, H. (2007). "A wideband electromagnetic micro power generator for wireless Microsystems," *IEEE, The 14th International Conference on Solid-State Sensors, Actuators and Microsystems*, pp. 275-278, 2007.
- Savage, H. T. and Spano, M. L. (1982). "Theory and application of highly magnetoelastic Metglas 2605SC," *Journal of Applied Physics*. 1982; 53(11):8092-8097.
- Shahruz, S.M. and Yi, J. (2007). "Performance of mechanical band-pass filters used in energy scavenging in the presence of fabrication errors and coupling," *Proc. IMECE 2007, ASME Int. Mechanical Engineering Congress and Exposition*, pp.1-9, 2007.
- Shahruz, S.M. (2006). "Design of mechanical band-pass filters for energy scavenging," *Elsevier Ltd, Journal of Sound and Vibration* 292 (2006) 987-998.
- Shearwood, C. and Yates, R. B. (1997). "Development of an electromagnetic micro-generator," *Electron. Lett.* **33** 1883–4, 1997.
- Scherrer, S., Plumlee, D. G. and Moll, A. J. (2005). "Energy scavenging device in LTCC materials," *IEEE Workshop on Microelectronics and Electron Devices, WMED '05* pp 77–8, 2005.
- Simetric, (2009). http://www.simetric.co.uk/si_metals.htm, 2009.
- Sodano, H. A., Magliula, E. A., Park, G. and Inman, D. J. (2002). "Electric power generation using piezoelectric materials," *Proc. 13th Int. Conf. on Adaptive Structures and Technologies (Potsdam, Germany)* pp 153–61, 2002.
- Sodano, H. A., Inman, D. J., and Park, G. (2004). "A review of power harvesting using piezoelectric materials," *Shock Vib. Digest*, vol. 36, No. 3, May 2004 197–205.

- Soliman, M.S.M., Abdel-Rahman, E.M., El-Saadany, E.F. and Mansour, R.R. (2008). "A wideband vibration-based energy harvester," IOP Publishing, *Journal of Micromech. Microeng.* 18 (2008) 11 5021.
- Starner, T. (1996). "Human powered wearable computing," *IBM Syst. J.*, vol. 35, no. 3-4, pp. 618-629, 1996.
- Starner, T. and Paradiso, J. A. (2004). "Human generated power for mobile electronics," in *Low-Power Electronics Design*, C. Piquet, Ed. Boca Raton, FL: CRC Press, 2004, pp. 1-35.
- Stephen, N. G. (2006). "On energy harvesting from ambient vibration," *Journal of Sound and Vibration* 293 (2006) 409-425.
- Tashiro, R., Kabei, N., Katayama, K., Ishizuka, Y., Tsuboi, F., and Tsuchiya, K. (2002). "Development of an electrostatic generator that harnesses the ventricular wall motion," *Jpn. Soc. Artif. Organs*, vol. 5, pp. 239-245, 2002.
- Thomson, W. T., and Dahleh, M. D. (1998). *Theory of Vibration with Applications*, Prentice Hall, Upper Saddle River, N.J, 1998.
- Torah, R. N., Beeby, S. P., T. J., O'Donnell, T. and Roy, S. (2006). "Development of a cantilever beam generator employing vibration energy harvesting," in *Proc. 6th Int. Workshop Micro Nanotechnol. Power Generation Energy Conversion Applicat.*, Berkeley, CA, pp. 181-184, 2006.
- Triplett, A., Quinn, D. D., Vakakis, A. F. and Bergman, L. A. (2009). "Energy harvesting from an impulsive load with essential nonlinearities," *ASME International Design Engineering Technical Conferences*, DETC2009-86669, 2009.
- Tseng, W. Y. (1970). *Nonlinear Vibrations of Straight and Buckled Beams under Harmonic Excitation*," PhD. Thesis, 1970.
- Tseng, W. Y. and Dugundji, J. (1971). "Nonlinear vibrations of a buckled beam under harmonic excitation," *Journal of Applied Mechanics*, vol. 38, pp. 467-476, 1971.
- Umeda, M., Nakamura, K., and Ueha, S. (1996). "Analysis of the transformation of mechanical impact energy to electric energy using piezoelectric vibrator." *Japanese Journal of Applied Physics Part 1- Regular Papers Short Notes & Review Papers*, 35(5B), 3267-3273, 1996.
- Vakakis, A. F., Manevitch, L. I., Gendelman, O., and Bergman, L. (2003). "Dynamics of linear discrete systems connected to local, essentially non-linear attachments," *J. Sound Vib.*, 264, pp. 559-577, 2003.
- Vetorino, S.R. et al. (2001). *Renewable Energy Flashlight*, US patent 6,220,719, to Applied Innovative Technologies, Inc., Patent and Trademark Office, 2001.
- Wang, L. (2007). *Vibration Energy Harvesting by Magnetostrictive Material for Powering Wireless Sensors*, PhD. Thesis, 2007.
- Wang, L. and Yuan, F. G. (2008). "Vibration energy harvesting by magnetostrictive material," *Smart Material and Structure* 17 (2008) 045009.

Williams, C.B, and Yates, R.B. (1995). "Analysis of a micro-electric generator for Microsystems," *Transducers 95/Eurosensors IX*, (1995)369 – 372.

Williams, C. W., Woods, R. C. and Yates, R. B. (1996). "Feasibility of a vibration powered micro-electric generator," *IEE Coll. On Compact Power Sources (London)* 7/1–7/3, 1996.

Williams, C.B., Shearwood, S., Harradine, M.A., Mellor, P.H., Birch, T.S. and Yates, R.B. (2001), "Development of an electromagnetic micro-generator," *Proc. Inst. Elect. Eng. Circuits, Devices Syst.*, vol. 148, No. 6, pp. 337-342, 2001.

Wu, W-J, Chen, Y-F, Chen, Y-Y, Wang, C-S and Chen, Y-H, (2007). " Smart wireless sensor network powered by random ambient vibrations," *Proc. IEEE Int. Conf. on Systems, Man and Cybernetics (Taipei)*, pp2701-8, 2007.

Xing, X., Lou, J., Yang, G. M., Obi, O., Driscoll, C., and Sun, N. X. (2009). "Wideband vibration energy harvester with high permeability magnetic Material," *Applied Physics Letters* 95(2009), 134103.

Appendix